

Systematics of 2^+ states in C isotopes from the no-core shell model

C. Forssén,^{1,*} R. Roth,² and P. Navrátil³

¹*Fundamental Physics, Chalmers University of Technology, 412 96 Göteborg, Sweden*

²*Institut für Kernphysik, Technische Universität Darmstadt, 64289 Darmstadt, Germany*

³*TRIUMF, 4004 Wesbrook Mall, Vancouver,*

British Columbia, V6T 2A3 Canada[†]

Lawrence Livermore National Laboratory,

P.O. Box 808, L-414, Livermore, CA 94551, USA

(Dated: October 8, 2018)

Abstract

We study low-lying states of even carbon isotopes in the range $A = 10 - 20$ within the large-scale no-core shell model (NCSM). Using several accurate nucleon-nucleon (NN) as well as NN plus three-nucleon (NNN) interactions, we calculate excitation energies of the lowest 2^+ state, the electromagnetic $B(E2; 2_1^+ \rightarrow 0_1^+)$ transition rates, the 2_1^+ quadrupole moments as well as selected electromagnetic transitions among other states. Recent experimental campaigns to measure 2^+ -state lifetimes indicate an interesting evolution of nuclear structure that pose a challenge to reproduce theoretically from first principles. Our calculations do not include any effective charges or other fitting parameters. However, calculated results extrapolated to infinite model spaces are also presented. The model-dependence of those results is discussed. Overall, we find a good agreement with the experimentally observed trends, although our extrapolated $B(E2; 2_1^+ \rightarrow 0_1^+)$ value for ^{16}C is lower compared to the most recent measurements. Relative transition strengths from higher excited states are investigated and the influence of NNN forces is discussed. In particular for ^{16}C we find a remarkable sensitivity of the transition rates from higher excited states to the details of the nuclear interactions.

PACS numbers: 21.60.De, 21.10.Tg, 21.10.Ky, 21.30.Fe, 27.20.+n, 27.30.+t

[†] Present address.

*christian.forssen@chalmers.se

I. INTRODUCTION

Electric quadrupole (E2) matrix elements are important quantities in probing nuclear structure. In particular, they are very sensitive to nuclear deformation, the decoupling of proton and neutron degrees of freedom, and they are often affected by small components of the nuclear wave functions. In this paper we perform systematic studies of observables obtained from diagonal and non-diagonal E2 matrix elements for even carbon isotopes, from ^{10}C to the very neutron rich ^{20}C . Quadrupole moments, corresponding to diagonal E2 matrix elements, are inherently difficult to measure for excited 2^+ states. Off-diagonal matrix elements, however, have recently been studied for several unstable carbon isotopes using lifetime measurements [1–6]. In this way, the reduced transition probability, $B(E2; 2_1^+ \rightarrow 0_1^+)$, can be extracted since it's inversely proportional to the lifetime of the 2^+ state. As a result of these experimental studies, different claims have been made on the nuclear structure in this chain of isotopes. Initial excitement was triggered by the observation of a strongly quenched E2 transition in ^{16}C [2]. Based on the liquid-drop model, which predicts the $B(E2)$ to be inversely proportional to the 2^+ excitation energy, Imai *et al.* [2] claimed an anomalous reduction of the E2 strength when comparing 2^+ lifetimes for ^{14}C ($E_{2^+} = 7.01$ MeV) and ^{16}C ($E_{2^+} = 1.77$ MeV). However, the $^{16}\text{C}(2^+)$ lifetime was remeasured by Wiedeking *et al.* [3] providing a much shorter value, thus indicating a larger $B(E2)$ strength. Their results were analyzed in terms of shell-model calculations. Adjusting the effective neutron charge to reproduce their measured lifetimes they made the claim that the results for ^{16}C are “normal” to this region. Lifetime measurements of $^{16,18}\text{C}$ were reported by Ong *et al.* [4]. The presented results for ^{16}C came from a reanalysis of the original data [2], now giving a larger but still quenched $B(E2)$ strength, while the new ^{18}C data indicated the persistence of the quenching of E2 strengths in heavy carbon isotopes. Possible explanations were put forward in terms of the decoupling of protons and neutrons resulting in very low values for the neutron effective charges and/or the appearance of a new proton magic number $Z = 6$ in this region. Some of these statements were backed up by new shell-model calculations by Fujii *et al.* [7] reproducing the $^{16,18}\text{C}$ results employing exceptionally small effective charges. An alternative explanation in terms of core polarization effects was recently proposed by Ma *et al.* [8]. They used a microscopic particle-vibration approach to compute core polarization effects on valence nucleons. In contrast with empirical effective charges, usually employed

in shell-model calculations, they noted a very strong quenching from core polarization on *sd*-shell neutrons for heavy carbon isotopes.

These various developments provide a strong motivation to perform large-scale calculations, with realistic interactions, to study the evolving nuclear structure in the carbon chain of (even) isotopes with particular focus on 2^+ states and quadrupole moments. We have, therefore, carried out no-core shell model (NCSM) [9, 10] calculations for low-lying states of the even-even carbon isotopes with $A = 10-20$. As described in more detail below, these calculations are performed starting from realistic Hamiltonians without adjustable parameters. In particular, since our many-body scheme does not involve an inert-core approximation we use bare charges when evaluating electromagnetic observables.

A. Theoretical formalism

The NCSM method has been described in great detail in several papers, see e.g., Refs. [10, 11]. Here, we just outline the approach as it is applied in the present study. We start from the intrinsic Hamiltonian for the A -nucleon system $H_A = \mathcal{T}_{\text{rel}} + \mathcal{V}$, where \mathcal{T}_{rel} is the relative kinetic energy and \mathcal{V} is the sum of nuclear and Coulomb interactions. The potential term will always contain two-body operators, but we can also include three-body terms originating from an initial NNN force, or three-body terms induced by a unitary transformation of the Hamiltonian. This transformation, further described below, is employed to soften the Hamiltonian for use in a truncated many-body basis.

In this work we have used several different nuclear potentials. Common to all of them is that they reproduce NN phase shifts with very high precision. First we have two pure NN interactions: CD-Bonn 2000 [12] (CDB2k), based on one-boson exchange theory, and INOY [13] that introduces a nonlocality to include some effects of three-nucleon forces. The latter is fitted also to three-nucleon observables. In addition, we have used the most recent chiral NN plus NNN interaction, i.e. the $N^3\text{LO}$ NN interaction of Ref. [14] and a local chiral $N^2\text{LO}$ NNN potential with low-energy constants determined entirely in the three-nucleon system [15]. The regulator cutoff energy of these chiral potentials is 500 MeV.

We solve the many-body problem in a large but finite harmonic-oscillator (HO) basis truncated by a maximal total HO energy of the A -nucleon system. The many-body model space is usually characterized by the truncation parameter N_{max} , giving the maximum num-

ber of HO excitations above the unperturbed A -nucleon ground state. The diagonalization of the Hamiltonian in this many-body basis is a highly non-trivial problem because of the very large dimensions that is encountered. To solve this problem, we have used a specialized version of the shell model code ANTOINE [16], adapted to the NCSM [17]. For the runs involving explicit NNN interactions we used the NCSD code [18] as well as the NSUITE package [19, 20], which is also capable of performing the importance-truncated NCSM calculations described below.

Due to the strong short-range correlations generated by the NN potentials, we usually compute an effective interaction to speed up the convergence. Two different similarity transformations have been used to construct the effective interactions: For CDB2k and INOY as initial NN interactions we compute two-body effective interactions appropriate to the low-energy basis truncation by a unitary transformation in the two-nucleon HO basis (Okubo-Lee-Suzuki effective interaction [9, 21, 22]). We note that the approximation of performing the transformation in two-body space, hence neglecting effective many-body terms, will actually disappear in the infinite model-space limit. For the chiral $NN+NNN$ Hamiltonian we employ the similarity renormalization group (SRG) with the initial and induced three-body terms included consistently [20, 23]. Induced four-body terms are neglected, and have actually been shown to give non-negligible contributions to ground-state energies in heavy p -shell nuclei [20]. Note also that we will not apply the unitary transformation to other operators than the Hamiltonian. In particular, results from long-range operators such as $E2$ are not expected to be much affected by this transformation [24, 25].

Dealing with systems having up to 20 nucleons it is a challenging task. To push beyond the full N_{max} -space limit we employ the importance-truncated (IT) NCSM scheme [19, 26]. It makes use of the fact that many of the basis states are irrelevant for the description of a set of low-lying states. Based on many-body perturbation theory, one can define a measure for the importance of individual basis states and discard states with an importance measure below a threshold value, thus reducing the dimension of the matrix eigenvalue problem. Through a sequence of IT calculations for different thresholds and an a posteriori extrapolation of all observables to vanishing threshold, we can recover the full NCSM results up to extrapolation errors [19].

II. RESULTS

A. Convergence and finite model-space results

The largest model spaces that we are able to reach in the full N_{max} -space NCSM calculations span from $N_{\text{max}} = 10$ in ^{10}C , via $N_{\text{max}} = 8$ in $^{12,14}\text{C}$, to $N_{\text{max}} = 6$ in $^{16,18}\text{C}$ and $N_{\text{max}} = 4$ in ^{20}C . The largest matrix dimension was $D = 1.4 \times 10^9$ for ^{18}C . However, using the IT-NCSM scheme we are able to obtain results also with $N_{\text{max}} = 8$ for $^{16,18}\text{C}$ and $N_{\text{max}} = 6$ for ^{20}C .

Our results exhibit dependence on N_{max} and $\hbar\Omega$ that should disappear once a complete convergence is reached. For our detailed studies of observables we are looking for the regions in which the N_{max} -convergence is the fastest and the dependence on $\hbar\Omega$ is the smallest. This optimal frequency range can vary between different observables and different isotopes. We will use the N_{max} -dependence of the binding energy in the largest model spaces as our primary criterion for selecting the optimal frequency range. From plots such as the left panels of Fig. 1, focusing in particular on the trend for large model spaces, we find that the $\hbar\Omega$ -range 10-14 MeV is optimal for all considered observables using the CDB2k-interaction and for the whole range of carbon isotope.

We note that relative energies, such as the excitation energy of the 2^+ state, are well converged, with the possible exception of the ^{14}C 2^+ energy. The extraction of energies is not the prime concern of this paper. In any case, it is clear that the CDB2k potential will underbind these isotopes. Still, we can hope that energy difference, i.e. excitation energies, are relatively well reproduced. As a rough estimate we can estimate the uncertainty ΔE of our results by observing the rates of convergence with respect to model-space size and HO frequency, respectively. Such error bars are obtained using the scheme of Ref. [27], and shown in a comparison of experimental data with NCSM calculated binding energies and 2^+ excitation energies of $^{10-20}\text{C}$ in Fig. 2. It is clear that the CDB2k interaction underbinds these isotopes by 10-20 % while the INOY interaction provides additional binding. The positive two-neutron separation energy for ^{16}C is not reproduced with any of these two realistic NN interactions. However, the many-body HO basis still provides a bound-state approximation to these states, and the additional binding provided, e.g., by NNN interactions will not necessarily change their structure (see the discussion in Sec. IID). We note

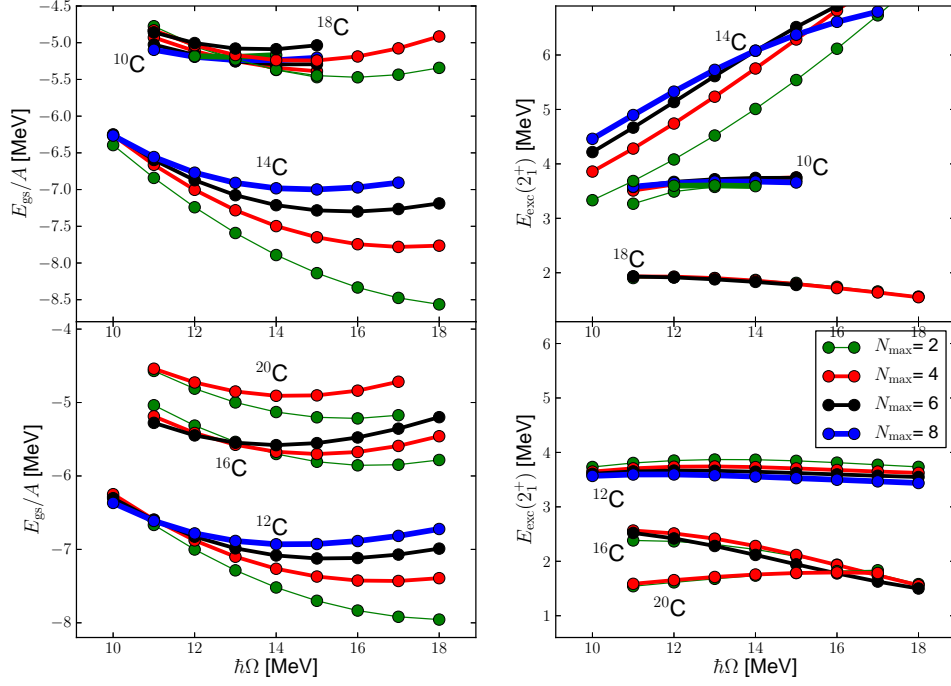


FIG. 1: (Color online) $\hbar\Omega$ -dependence for the ground-state energy (presented as E_{gs}/A) and the first 2^+ excitation energy for $^{10-20}\text{C}$. Results are obtained using the CDB2k interaction and each curve corresponds to a particular model space represented by the truncation parameter N_{max} .

that excitation energies are well converged, and we find a very good agreement with the experimental trend. The possible exception is the large 2_1^+ excitation energy of ^{14}C that is over-predicted with the INOY interaction.

We focus next on electric quadrupole moments, both diagonal and off-diagonal (transition strengths). Our full N_{max} -space results are shown in Figs. 3,4 (filled symbols) together with IT-NCSM results (open symbols). The data is plotted as a function of $1/N_{\text{max}}$ for the selected range of HO frequencies. Infinite model space corresponds to $1/N_{\text{max}} \rightarrow 0$.

A reliable extrapolation to infinite model space would be still more useful. Extrapolation schemes, in particular for quadrupole observables, are introduced and discussed in more detail in the next section.

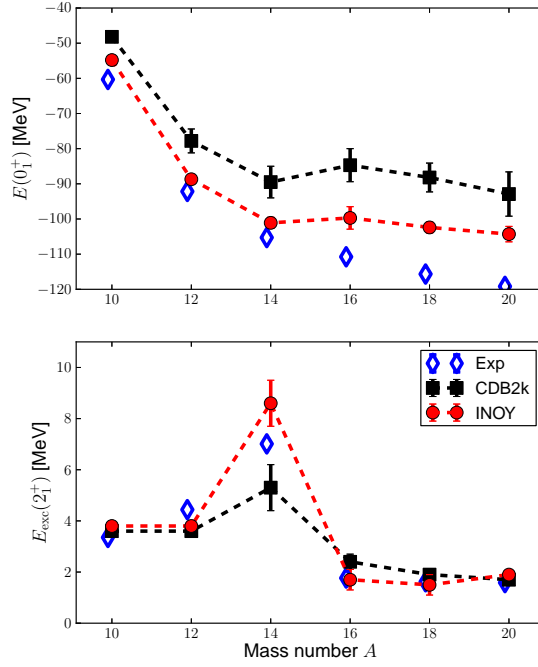


FIG. 2: (Color online) NCSM calculated binding energies and 2^+ excitation energies of $^{10-20}\text{C}$ compared with experimental results.

B. Extrapolation to infinite model space

Working in a large many-body HO basis facilitates the implementation of relevant symmetries and enables us to capture the important physics of the realistic nuclear interactions that are employed in our *ab initio* approach to nuclear structure. However, the need to truncate our model space introduces constraints on our ability to describe very short-distance (high energy) as well as long-distance correlations. This fact was recently expressed in terms of various definitions of infrared (IR) and ultraviolet (UV) cutoffs in finite HO bases [28, 29]. Suggestions on how to employ these model-space parameters to extrapolate to infinite model space were proposed.

Common to all extrapolation schemes is the need to introduce a number of fit parameters to extrapolate the *ab initio* results to the infinite space. Using the insights offered by introducing UV and IR regulators rather than model-space parameters N_{max} and $\hbar\Omega$, the number of free parameters can be significantly reduced. In general, extrapolations based on pure phenomenology have more fit parameters [27, 30, 31]. Dealing with Okubo-Lee-Suzuki

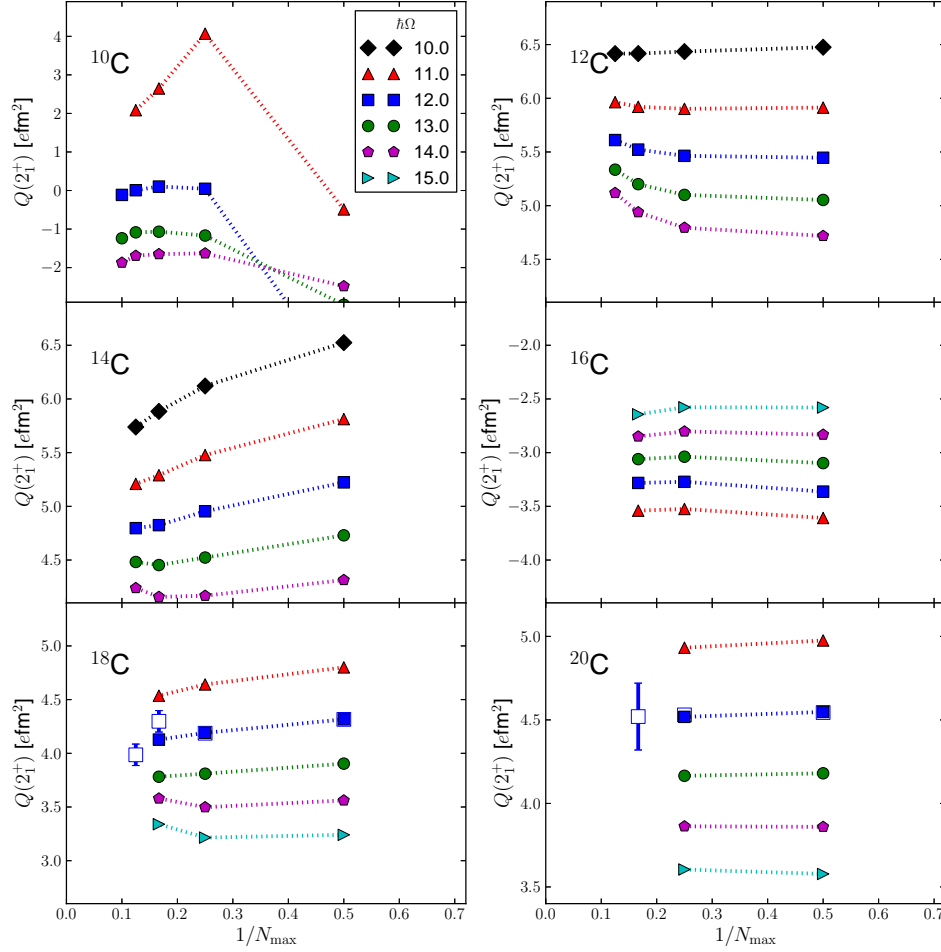


FIG. 3: (Color online) NCSM calculated electric quadrupole moments of the first 2^+ states in $^{10-20}\text{C}$. Results obtained with the CDB2k NN potential are presented. Filled (open) symbols correspond to full (importance-truncated) space results. See also Table I.

transformed results, for which the Hamiltonian is *model-space dependent* and the variational principle does not apply, our experience is that multiparameter fits seem to be necessary.

We focus here on our results for electric quadrupole observables. In Figs. 3,4 we show our full (importance-truncated) N_{max} -space NCSM results as filled (open) symbols for various HO frequencies. As observed, they exhibit dependence on N_{max} and $\hbar\Omega$. We know that, by construction, this dependence should disappear once a complete convergence is reached. This implies that N_{max} -sequences obtained at different HO frequencies should all converge

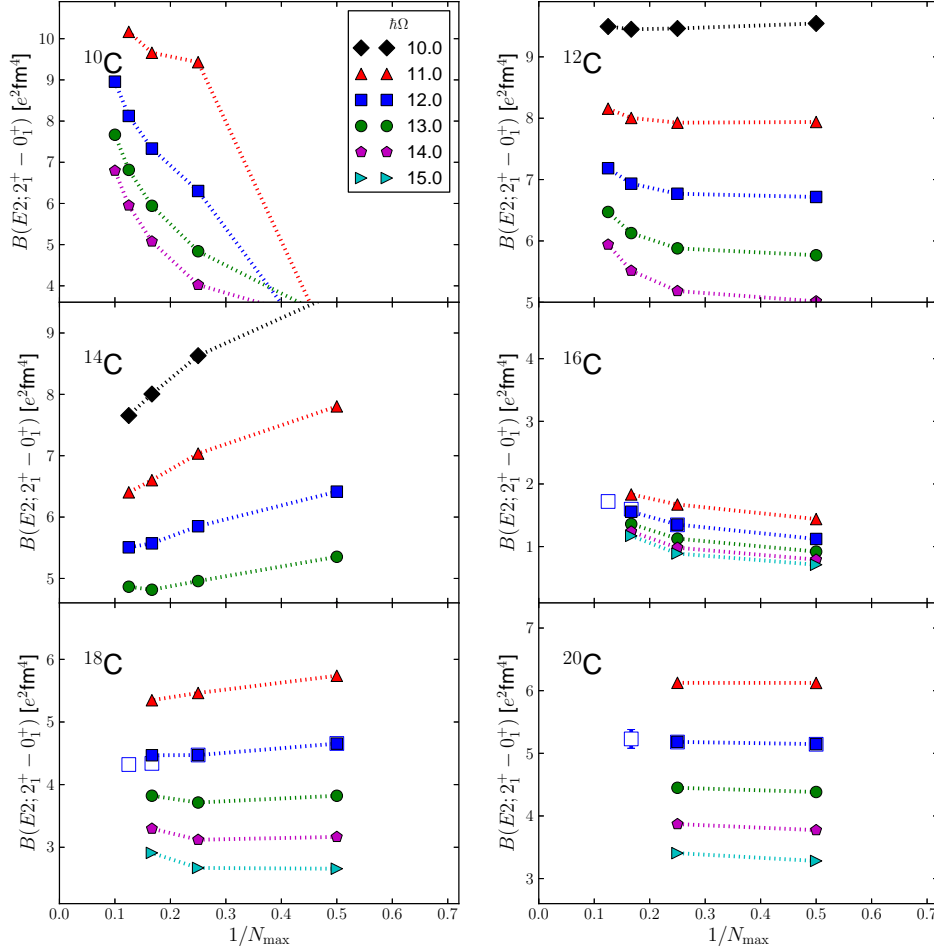


FIG. 4: (Color online) NCSM calculated $B(E2; 2_1^+ \rightarrow 0_1^+)$ strengths in $^{10-20}\text{C}$. Results obtained with the CDB2k NN potential are presented. Filled (open) symbols correspond to full (importance-truncated) space results. See also Table I.

to the same result. This feature can be utilized to perform a constrained fit to multiple sequences [27, 31]. To this end, we use as large an N_{max} basis as feasible for a wide range of HO frequencies, and extrapolate calculated observables to infinite space. Results obtained for a range of frequencies are used in the fits. We find that the convergence behavior for E2 observables, as a function of N_{max} , can be rather well fitted by: $q = q_{\infty} + c_0/N_{\text{max}} + c_1/N_{\text{max}}^2$. The parameters c_0 and c_1 are allowed to vary for each $\hbar\Omega$ -sequence, while the single parameter q_{∞} gives the extrapolated result at $N_{\text{max}} \rightarrow \infty$. Typically we use a range

of five HO frequencies for these constrained fits. Finally, an error estimate is made based on repeating the constrained fit keeping various subsets (pairs and triples) of frequencies in the selected range.

In addition, we perform an additional, simplified, extrapolation procedure using simple first-degree polynomials in $1/N_{\text{max}}$: $q = c_0 + c_1/N_{\text{max}}$. This allows simple fits to pairs of data $(q_{\hbar\Omega, N_{\text{max}}}, q_{\hbar\Omega, N_{\text{max}}-2})$. Using a sequence of such fits (for different values of $\hbar\Omega$) gives a range of c_0 parameters that together provides an estimate for the range of the desired observable q_∞ . As we follow the convergence with increasing model space sizes: $N_{\text{max}} = (8, 6), (6, 4), (4, 2)$, we expect to see that this range gets smaller and smaller.

Figure 5 shows several examples of the extrapolation procedures for quadrupole moments and $B(\text{E2})$ strengths. The data is the same as in Figs. 3,4. The results are plotted as a function of $1/N_{\text{max}}$ for the selected range of HO frequencies. The dashed lines correspond to the constrained fits to five $\hbar\Omega$ -sequences. The bars correspond to the ranges from the linear extrapolations. Starting from the right we have $N_{\text{max}} = (4, 2), (6, 4), (8, 6)$. Numerical results for E2 observables for all isotopes are presented in Table I. The range that is presented from the linear fit corresponds to the largest N_{max} that was reached for that particular isotope. We note that the use of a range of frequencies usually include sequences that converge from above and from below. This allows a more precise determination of the extrapolated, final result. A particular exception to this behavior is the $B(\text{E2})$ strength of ^{16}C , for which all sequences converge from below. This will be further commented below.

C. Systematics of electric quadrupole observables

We focus now in particular on a discussion of the systematics of E2 observables in the chain of even carbon isotopes. First, we note that no extrapolation was performed for the energy observables presented in Fig. 2, although the magnitude of the $\hbar\Omega$ - and N_{max} -dependence was indicated by the error bars. However, as discussed in the previous section, a number of fit parameters are introduced in the extrapolation of results for E2 observables to infinite model space. In Fig. 6 we compare the extrapolated theoretical results (linear fit) with the experimental trends for the carbon chain of isotopes. Numerical, extrapolated results, for both extrapolation schemes, are presented in Table I. It is obvious from Fig. 6 that our calculated $B(\text{E2}; 2_1^+ \rightarrow 0_1^+)$ agrees rather well with the most recent experimental

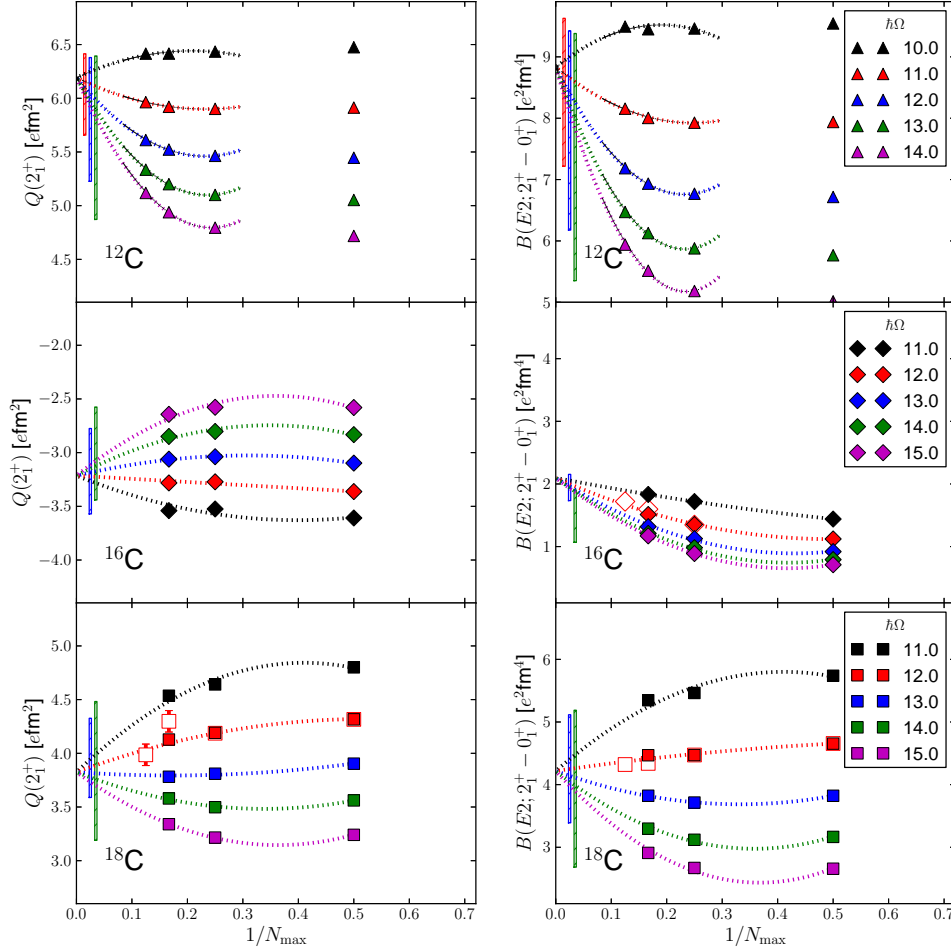


FIG. 5: (Color online) Model-space dependence of calculated E2 observables for $^{12,16,18}\text{C}$ in the NCSM. Results obtained with the CDB2k NN potential are presented as a function of $1/N_{\text{max}}$. Filled (open) symbols correspond to full (importance-truncated) space results. Dotted lines correspond to constrained fits, and the bars correspond to linear fits as described in the text. See also Table I.

data for the entire chain of isotopes.

We note that the extrapolation of our ^{16}C $B(E2; 2_1^+ \rightarrow 0_1^+)$ results is particularly difficult. Unlike the trends for other carbon isotopes, the $B(E2)$ value increases with N_{max} in the whole investigated HO frequency range (see Fig 5). This makes the upper bound less constrained. As a consequence, for this case we introduce a systematic error to bring the total uncertainty

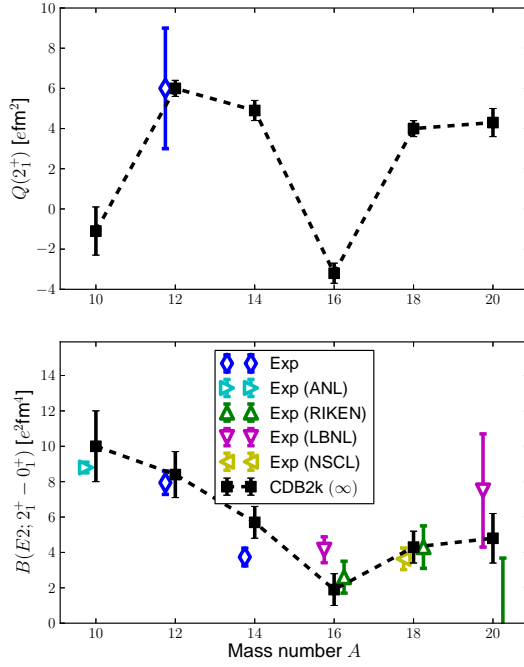


FIG. 6: (Color online) NCSM calculated E2 observables of $^{10-20}\text{C}$ compared with experimental results. See also Table I. NCSM results are obtained from linear extrapolations in $1/nm$ (see text for details).

to $\pm 0.9 e^2fm^4$ in accord with the neighbouring isotopes. Our final recommended value is below the most recent experimental results from LBNL [3, 36]. Furthermore, we note that our calculated quadrupole moment for the first 2^+ state of ^{16}C is $Q \approx -3.2 efm^2$ while for $A = 12, 14, 18, 20$ we find the quadrupole moment of the 2_1^+ state to be positive. Concerning the quadrupole moment of ^{18}C we find that the threshold-extrapolation of this observable in the IT-NCSM has a comparatively large uncertainty, which shows up in the sizeable errorbars shown in the plot.

A qualitative understanding of these findings can be obtained by studying the mean occupation numbers of different single-particle states in the NCSM wave functions. In Fig. 7 these occupancies are plotted for the ground- and first 2^+ -state for the whole range of carbon isotopes. For comparison we show the ground-state occupation numbers that are expected in an unperturbed shell model (non-interacting particles). We show explicitly the occupation numbers up to the sd shell. Not shown, however, are occupation numbers for the fp shell and beyond. They extend up to 0.01–0.11 for both protons and neutrons.

TABLE I: NCSM calculated E2 observables of $^{10-20}\text{C}$ compared with experimental results. NCSM results are obtained using the CDB2k interaction. The recommended values are obtained from two different extrapolation schemes: simple linear (lin.) and constrained fits (cons.) to sequences of $\hbar\Omega$ -frequencies (see text for details).

	$Q(2_1^+) [\text{efm}^2]$			Refs.
	Th. (cons. fit)	Th. (lin. fit)	Exp.	
^{10}C	-1.1 ± 1.2^a	—	—	[32]
^{12}C	$+6.2 \pm 0.2$	$+6.0 \pm 0.4$	$+6 \pm 3$	
^{14}C	$+4.7 \pm 0.4$	$+4.9 \pm 0.5$	—	
^{16}C	-3.2 ± 0.3	-3.2 ± 0.5	—	
^{18}C	$+3.8 \pm 0.2$	$+4.0 \pm 0.4$	—	
^{20}C	$+4.3 \pm 0.6$	$+4.3 \pm 0.7$	—	
	$B(\text{E2}; 2_1^+ \rightarrow 0_1^+) [e^2\text{fm}^4]$			Refs.
	Th. (cons. fit)	Th. (lin. fit)	Exp.	
^{10}C	10 ± 2^a	—	8.8 ± 0.3	[1]
^{12}C	8.8 ± 0.7	8.4 ± 1.3	7.59 ± 0.42	[33]
^{14}C	5.3 ± 0.7	5.7 ± 0.9	3.74 ± 0.50	[34]
^{16}C	2.2 ± 0.9	1.9 ± 0.9	$2.6 \pm 0.9, 4.15 \pm 0.73$	[3, 4]
^{18}C	4.2 ± 0.4	4.3 ± 0.9	$4.3 \pm 1.2, 3.64^{+0.55}_{-0.61}$	[4, 35]
^{20}C	4.8 ± 1.1	4.8 ± 1.4	$< 5.7, 7.5^{+3.2}_{-1.8}$	[5, 6]

^aStrong mixing of the first two 2^+ states. The estimate of ^{10}C E2 observables is obtained by studying the sums and ratios of results for both 2^+ states.

The excitation mechanisms are quite obvious for $^{14,16}\text{C}$. In ^{14}C the 2_1^+ state corresponds to a proton excitation within the p shell, while in ^{16}C the 2_1^+ state is obtained through a re-configuration of neutrons in the sd shell. The value of the $B(\text{E2})$, for this particular case, will be quite sensitive to the fine details of the re-configuration. Energy observables, on the other hand, are not as sensitive to these small nuclear-structure details and can therefore be expected to converge faster than the $B(\text{E2})$.

For ^{10}C we observe a very strong mixing of the first two 2^+ states using the CDB2k

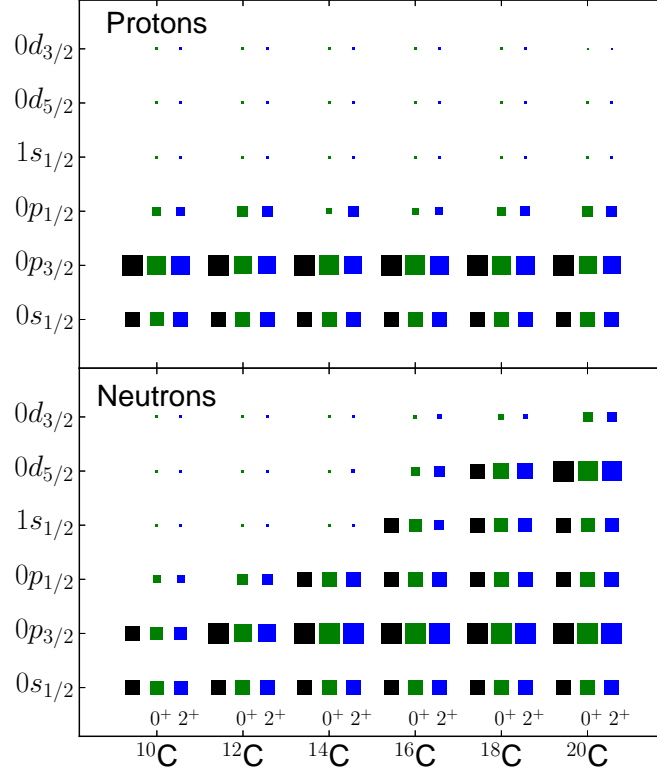


FIG. 7: (Color online) Occupation numbers for the ground- (middle, green squares) and first 2^+ -state (right, blue squares) in $^{10-20}\text{C}$ obtained with the CDB2k interaction. The area of the squares are proportional to the occupation numbers and can be compared with the unperturbed ground-state, shell-model occupation numbers (left, black squares). We can note in particular the proton (neutron) excitation character of the ^{14}C (^{16}C) 2^+ state.

interaction at small frequencies. To get at least crude estimates of the E2 properties of the 2_1^+ state we used a slightly different extrapolation approach: The ratios of, e.g., $Q(2_1^+)$ and $Q(2_2^+)$ was plotted for larger frequencies where the mixing is not observed, while the sum was plotted for the full range of frequencies. From such plots, for Q and $B(\text{E2})$ observables, we can deduce estimates for $Q(2_1^+)$ and $B(\text{E2}; 2_1^+ \rightarrow 0_1^+)$ and their uncertainties. These are included in Table I and Fig. 6.

We note that the different NN interactions used in this study give very similar isotopic trends for E2 observables, but with a consistently smaller magnitude for the INOY interac-

TABLE II: Relative $B(E2)$ values for transitions among excited states of $^{14-20}\text{C}$. Results obtained in full N_{max} -space at fixed HO-frequency with the CDB2k ($\hbar\Omega = 12$ MeV) and INOY ($\hbar\Omega = 17 - 18$ MeV) NN interactions are compared. $N_{\text{max}} = 6$ for $^{14-18}\text{C}$ and $N_{\text{max}} = 4$ for ^{20}C .

A	$\frac{B(E2; 2_2^+ \rightarrow 0_1^+)}{B(E2; 2_1^+ \rightarrow 0_1^+)}$		$\frac{B(E2; 2_2^+ \rightarrow 2_1^+)}{B(E2; 2_1^+ \rightarrow 0_1^+)}$	
	CDB2k	INOY	CDB2k	INOY
14	0.001	0.000	0.48	0.81
16	2.2	0.30	2.0	0.79
18	0.046	0.22 ^a	0.029	1.7 ^a
20	0.017	0.035	0.12	0.28

^aFor this particular interaction we observe considerable mixing between two 2^+ states, with different structure, for certain choices of the HO frequency. These results are for $\hbar\Omega = 18$ MeV.

tion. This observation is connected to the anomalously large nuclear density generated by this interaction found already in ^4He calculations [37, 38].

Finally, a study of the characteristics of the second 2^+ state in these isotopes strengthens the conclusion of the prominence of ^{16}C in the structural evolution of the chain of even carbon isotopes. The sign of the quadrupole moment of this state, $Q(2_2^+)$, is reversed from $Q(2_1^+)$. I.e., it's negative for all isotopes except for ^{16}C (and possible ^{10}C). In addition, as summarized in Table II, the relative $B(E2)$ strength from this second 2^+ state to the ground state is much smaller than that from the first 2^+ for all isotopes but ^{16}C . These findings are obtained with both NN Hamiltonians used in this study. However, the relative transitions from the second 2^+ in $^{16,18}\text{C}$ stand out with clear differences in the predictions of CDB2k and INOY, see Table II. Note, however, that the convergence of the second 2^+ state is computationally more difficult, and therefore the statements on relative transition strengths are based on runs performed at a single HO frequency. For ^{18}C , in particular, there is a strong $\hbar\Omega$ -dependence for the INOY results that makes the corresponding claim of a strong $2_2^+ \rightarrow 2_1^+$ E2 transition less robust. For ^{16}C , however, the interaction dependence is solid and intriguing. As the INOY interaction often hints to possible structural influence from NNN forces we continue our study in the next section with a more detailed investigation of the ^{16}C structure using Hamiltonians with realistic NNN terms.

D. Higher-lying states of ^{16}C and the role of the NNN interaction

Transitions from higher excited states of ^{16}C were studied in a recent experiment [36]. In particular, the transitions $2_2^+ \rightarrow 2_1^+$, $4_1^+ \rightarrow 2_1^+$ and $3_1^+ \rightarrow 2_1^+$ were observed. Interestingly, no transition from the 2_2^+ state to the ground state was seen. We performed additional calculations with different Hamiltonians to study higher excited states in ^{16}C and their electromagnetic transitions. In Fig. 8, we show the calculated and experimental energy levels of ^{16}C , and in Table III we summarize our calculated $B(E2)$ values among excited states normalized to $B(E2; 2_1^+ \rightarrow 0_1^+)$. In particular, we compare results obtained with SRG-transformed chiral NN and chiral $NN+NNN$ interactions (including the SRG-induced three-nucleon terms in both cases as discussed in Ref. [20]) calculated in the IT-NCSM, to those obtained with the two-body effective CDB2k interaction. A striking feature is a strong suppression of the $2_2^+ \rightarrow 0_1^+$ transition when the initial NNN interaction is included. The sensitivity to the presence of the NNN interaction is remarkable. The $2_2^+ \rightarrow 0_1^+$ transition is suppressed by a factor of ~ 7 in the calculation with the NNN compared to chiral NN only, and a factor of ~ 20 compared to CDB2k. Clearly, the calculation without the NNN interaction contradicts the new MSU experiment [36] where indeed the $2_2^+ \rightarrow 0_1^+$ transition was not observed. From Table III we observe that relative E2 transition strengths obtained with the chiral NN interaction are similar to the ones obtained with the CDB2k interaction. Furthermore, we see from Table II that the relative $B(E2)$ calculated with the INOY interaction (that mimics some NNN effects) resemble results of the chiral $NN+NNN$ Hamiltonian. The excitation energies of the five lowest ^{16}C excited states are also influenced by the NNN interaction as seen in Fig. 8. The agreement with the experimental spectrum is quite reasonable in all presented cases, although slightly improved in the calculation with the chiral $NN+NNN$ Hamiltonian.

From Table III, we also note a strong sensitivity of the $3_1^+ \rightarrow 2_1^+$ transition to the presence of the NNN interaction. The calculation with the chiral $NN+NNN$ Hamiltonian predicts a strongly suppressed $B(E2; 3_1^+ \rightarrow 2_1^+)$ transition. A transition between these states is observed, however [36]. Our calculation with the NNN interaction predicts this transition to be of M1 character as seen from Table IV. We also observe a sign change of the magnetic moments of both the 2_1^+ and the 2_2^+ states in calculations with the NNN interaction included. The magnetic moment of the 3_1^+ state is unaffected, however. The sensitivity of the 2_1^+

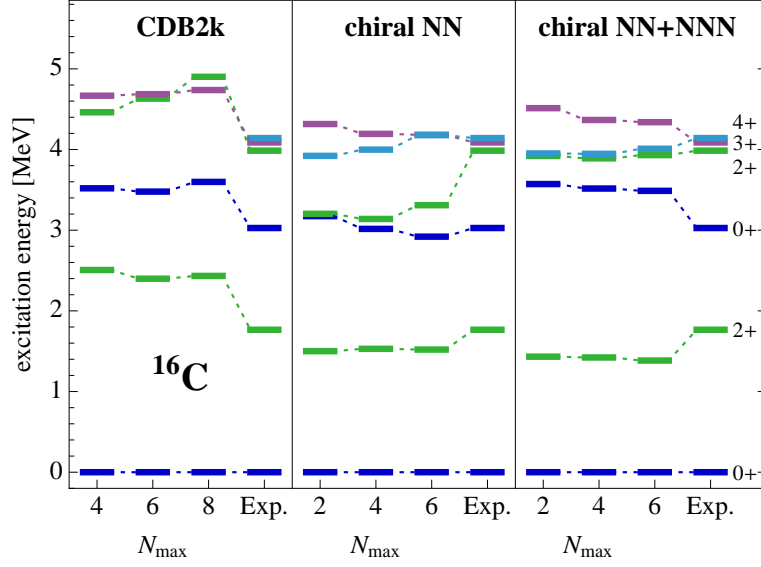


FIG. 8: (Color online) Excitation energies of the lowest states of ^{16}C . Calculations using the Okubo-Lee-Suzuki-transformed CDB2k potential at $\hbar\Omega = 12$ MeV (left) and the SRG-evolved chiral NN and $NN+NNN$ interactions with $\Lambda = 1.88 \text{ fm}^{-1}$ for $\hbar\Omega = 16$ MeV (middle and right) are compared to experiment for different values of N_{max} . The SRG-evolved chiral interactions include induced NNN terms.

magnetic moment to the NNN interaction we also find in ^{20}C (see Table IV).

Overall, we find a strong sensitivity of the electromagnetic observables in ^{16}C to the details of nuclear Hamiltonian. Note, however, that we don't employ two-body currents, and that these are expected to have a non-negligible influence on magnetic dipole moments. Furthermore, additional studies are needed regarding the effect of the similarity transformation on this type of operator. But the long-range quadrupole operator, that is the main target of this study, is not expected to be much affected by this transformation. We conclude that more detailed experimental study of higher excited states and their transitions will be very useful.

III. CONCLUSION

In summary, we have computed low-lying states of even carbon isotopes with $A = 10 - 20$ within the no-core shell model. We have used several accurate nucleon-nucleon (NN) as well as NN plus NNN interactions and calculated excitation energies of the lowest 2^+ state, the

TABLE III: Relative $B(E2)$ values for transitions among excited states of ^{16}C . Results obtained with the CDB2k NN potential, the chiral NN , and the chiral $NN+NNN$ interaction are compared. For CDB2k we use the Okubo-Lee-Suzuki effective interactions ($\hbar\Omega = 12$ MeV, $N_{\text{max}}=6$) and for the chiral interactions we use SRG-evolved interactions ($\Lambda = 1.88 \text{ fm}^{-1}$, $\hbar\Omega = 16$ MeV, $N_{\text{max}}=6$) including the induced three-nucleon terms.

$\frac{B(E2; J_i \rightarrow J_f)}{B(E2; 2_1^+ \rightarrow 0_1^+)}$	CDB2k	chiral NN	chiral $NN+NNN$
$2_1^+ \rightarrow 0_1^+$	1	1	1
$2_2^+ \rightarrow 0_1^+$	2.2	0.75	0.11
$2_2^+ \rightarrow 2_1^+$	2.0	1.7	0.65
$3_1^+ \rightarrow 2_1^+$	0.36	0.31	0.02
$4_1^+ \rightarrow 2_1^+$	0.89	0.69	0.80

TABLE IV: Magnetic dipole moments and $B(M1)$ transition strengths of excited states in $^{16,20}\text{C}$. Results obtained with the CDB2k NN potential and the SRG-evolved chiral $NN+NNN$ interaction are compared. $B(M1)$ in μ_N^2 and μ in μ_N . Parameters as in Table III with $N_{\text{max}}=4$ for ^{20}C . The brackets indicate the uncertainties of the threshold extrapolation for the IT-NCSM.

	^{16}C		^{20}C	
	CDB2k	chiral $NN+NNN$	CDB2k	chiral $NN+NNN$
$B(M1; 2_2^+ \rightarrow 2_1^+)$	0.013	0.063	0.015	
$B(M1; 3_1^+ \rightarrow 2_1^+)$	0.17	0.17	0.013	
$\mu(2_1^+)$	0.13	-0.42	0.22	0.001(8)
$\mu(2_2^+)$	1.3	-0.79	0.58	
$\mu(3_1^+)$	-3.2	-3.1	0.016	

electromagnetic $B(E2; 2_1^+ \rightarrow 0_1^+)$ transition strengths, the 2_1^+ quadrupole moments as well as selected electromagnetic transitions among higher excited states. We use a truncated many-body model space, which however can be systematically improved by increasing the cutoff. We employ two different similarity transformation schemes to adapt the Hamiltonian to the available model space. The calculations do not include effective charges or any other

fitting parameters. Note that the truncation of the many-body basis used in the NCSM should in principle be followed by a transformation of the transition operator that is consistent with the renormalization of the Hamiltonian. Regarding long-range operators, such as Q , this transformation is not expected to produce very different end results for calculated observables [24, 25]. In addition, the small uncertainty associated with the approximation of using bare operators is partly built into the error estimates that we obtain from using several values of $\hbar\Omega$ and N_{max} .

We have presented full N_{max} -space results for energies and quadrupole observables. In addition, we used two simple schemes to extrapolate the quadrupole results to infinite model spaces. Additional fitting parameters are introduced in these schemes that make extrapolated results non-*ab initio*.

Overall, we have found a consistent NCSM description of the $B(E2; 2_1^+ \rightarrow 0_1^+)$ dependence on the mass number for the whole carbon isotopic chain from $A = 10$ to 20. However, our extrapolated $B(E2; 2_1^+ \rightarrow 0_1^+)$ values for ^{16}C , with different Hamiltonians, all underestimate the most recent experimental measurements. A similar result was obtained by Ma *et al.* [8] in a phenomenological approach. They used a microscopic particle-vibration model to compute core polarization effects. In their picture the reduced $B(E2)$ strength in heavy carbon isotopes can be traced back in particular to a strong quenching from core polarization on sd -shell neutrons. In our approach, however, there is no such separation into core and valence degrees of freedom.

In addition, we found a remarkable sensitivity of the transition rates from higher excited states in ^{16}C to the details of the nuclear interactions. The chiral $NN + NNN$ interaction gives the excitation spectrum of ^{16}C in a slightly better agreement with experiment than the CDB2k NN potential and, furthermore, the former interaction predicts the suppression of the $2_2^+ \rightarrow 0_1^+$ transition in agreement with experimental observations. We found a strong sensitivity of the magnetic moments of the 2_1^+ state to the nuclear interaction in ^{16}C and ^{20}C and even more so for the 2_2^+ state in ^{16}C .

The extrapolated NCSM results predict sign changes of the 2_1^+ quadrupole moments between different carbon isotopes. In particular, we predict a negative quadrupole moment in ^{16}C , a very small quadrupole moment in ^{10}C and a $B(E2; 2_1^+ \rightarrow 0_1^+)$ value in ^{10}C that is about the same as that in ^{10}Be . In ^{12}C , we obtain $Q(2_1^+) = +6.0 \pm 0.4 \text{ efm}^2$. It will be worth measuring these moments in the future.

Acknowledgments

We would like to thank A. Macchiavelli, P. Fallon, M. Wiedeking, and M. Petri for many useful discussions. Support from the European Research Council under the FP7 (ERC grant agreement no. 240603), the Swedish Research Council (dnr. 2007-4078), the Deutsche Forschungsgemeinschaft through contract SFB 634, the Helmholtz International Center for FAIR (HIC for FAIR), and the BMBF (06DA9040I) is acknowledged. Support from the Natural Sciences and Engineering Research Council of Canada (NSERC) Grant No. 401945-2011 is acknowledged. TRIUMF receives funding via a contribution through the National Research Council Canada. Computing resources have been provided by the Jülich Supercomputing Centre and by LOEWE-CSC. Prepared in part by LLNL under Contract DE-AC52-07NA27344.

-
- [1] E. A. McCutchan, C. J. Lister, S. C. Pieper, R. B. Wiringa, D. Seweryniak, J. P. Greene, P. F. Bertone, M. P. Carpenter, C. J. Chiara, G. Gürdal, et al., Phys. Rev. C **86**, 014312 (2012).
 - [2] N. Imai, H. J. Ong, N. Aoi, H. Sakurai, K. Demichi, H. Kawasaki, H. Baba, Z. Dombrádi, Z. Elekes, N. Fukuda, et al., Phys. Rev. Lett. **92**, 62501 (2004).
 - [3] M. Wiedeking, P. Fallon, A. O. Macchiavelli, J. Gibelin, M. S. Basunia, R. M. Clark, M. Cromaz, M.-A. Deleplanque, S. Gros, H. B. Jeppesen, et al., Phys. Rev. Lett. **100**, 152501 (2008).
 - [4] H. J. Ong, N. Imai, D. Suzuki, H. Iwasaki, H. Sakurai, T. K. Onishi, M. K. Suzuki, S. Ota, S. Takeuchi, T. Nakao, et al., Phys. Rev. C **78**, 14308 (2008).
 - [5] Z. Elekes, Z. Dombrádi, T. Aiba, N. Aoi, H. Baba, D. Bemmerer, B. A. Brown, T. Furumoto, Z. Fülöp, N. Iwasa, et al., Phys. Rev. C **79**, 11302 (2009).
 - [6] M. Petri, P. Fallon, A. O. Macchiavelli, S. Paschalis, K. Starosta, T. Baugher, D. Bazin, L. Cartegni, R. M. Clark, H. L. Crawford, et al., Phys. Rev. Lett. **107**, 102501 (2011).
 - [7] S. Fujii, T. Mizusaki, T. Otsuka, T. Sebe, and A. Arima, Phys. Lett. B **650**, 9 (2007).
 - [8] H.-L. Ma, B.-G. Dong, and Y.-L. Yan, Phys. Lett. B **688**, 150 (2010).
 - [9] P. Navrátil, J. P. Vary, and B. R. Barrett, Phys. Rev. Lett. **84**, 5728 (2000).
 - [10] P. Navrátil, S. Quaglioni, I. Stetcu, and B. R. Barrett, J. Phys. G: Nucl. Part. Phys. **36**, 083101 (2009).

- [11] B. R. Barrett, P. Navrátil, and J. P. Vary, Prog. Part. Nucl. Phys. **69**, 131 (2013).
- [12] R. Machleidt, Phys. Rev. C **63**, 24001 (2001).
- [13] P. Doleschall, Phys. Rev. C **69**, 54001 (2004).
- [14] D. R. Entem and R. Machleidt, Phys. Rev. C **68**, 41001 (2003).
- [15] D. Gazit, S. Quaglioni, and P. Navrátil, Phys. Rev. Lett. **103**, 102502 (2009).
- [16] E. Caurier and F. Nowacki, Acta Phys. Pol. B **30**, 705 (1999).
- [17] E. Caurier, P. Navrátil, W. E. Ormand, and J. P. Vary, Phys. Rev. C **64**, 51301 (2001).
- [18] P. Navrátil (2011), unpublished.
- [19] R. Roth, Phys. Rev. C **79**, 64324 (2009).
- [20] R. Roth, J. Langhammer, A. Calci, S. Binder, and P. Navrátil, Phys. Rev. Lett. **107**, 72501 (2011).
- [21] K. Suzuki and S. Y. Lee, Prog. of Theor. Phys. **64**, 2091 (1980).
- [22] S. Okubo, Prog. Theor. Phys. **12**, 603 (1954).
- [23] E. D. Jurgenson, P. Navrátil, and R. J. Furnstahl, Phys. Rev. Lett. **103**, 82501 (2009).
- [24] I. Stetcu, B. R. Barrett, P. Navrátil, and J. P. Vary, Phys. Rev. C **71**, 44325 (2005).
- [25] E. Anderson, S. Bogner, R. Furnstahl, and R. Perry, Phys. Rev. C **82**, 054001 (2010).
- [26] R. Roth and P. Navrátil, Phys. Rev. Lett. **99**, 92501 (2007).
- [27] C. Forssén, E. Caurier, and P. Navrátil, Phys. Rev. C **79**, 21303 (2009).
- [28] S. A. Coon, M. I. Avetian, M. K. G. Kruse, U. van Kolck, P. Maris, and J. P. Vary, Phys. Rev. C **86**, 054002 (2012).
- [29] R. Furnstahl, G. Hagen, and T. Papenbrock, Phys. Rev. C **86**, 031301 (2012).
- [30] P. Maris, J. Vary, and A. Shirokov, Physical Review C **79**, 014308 (2009).
- [31] C. Forssén, J. P. Vary, E. Caurier, and P. Navrátil, Phys. Rev. C **77**, 24301 (2008).
- [32] W. Vermeer, M. Esat, J. Kuehner, R. Spear, A. Baxter, and S. Hinds, Phys. Lett. B **122**, 23 (1983).
- [33] F. Ajzenberg-Selove, Nucl. Phys. A **506**, 1 (1990).
- [34] H. Crannell, P. L. Hallowell, J. T. O'Brien, J. M. Finn, F. J. Kline, S. Penner, J. W. J. Lightbody, and S. P. Fivozinsky, in *Kakuriken Kenkyu Hokoku* (1972), vol. 5, international conference on nuclear structure studies using electron scattering and photoreaction.
- [35] P. Voss, T. Baugher, D. Bazin, R. Clark, H. Crawford, A. Dewald, P. Fallon, A. Gade, G. Grinyer, H. Iwasaki, et al., Phys. Rev. C **86**, 011303 (2012).

- [36] M. Petri, S. Paschalis, R. Clark, P. Fallon, A. Macchiavelli, K. Starosta, T. Baugher, D. Bazin, L. Cartegni, H. Crawford, et al., Phys. Rev. C **86**, 044329 (2012).
- [37] R. Lazauskas and J. Carbonell, Phys. Rev. C **70**, 44002 (2004).
- [38] E. Caurier and P. Navrátil, Phys. Rev. C **73**, 21302 (2006).